Analysis of Internally Shunted Josephson Junctions

Original
Analysis of Internally Shunted Josephson Junctions / Lacquaniti, Vincenzo; Cassiago, Cristina; DE LEO, Maria; Fretto, MATTEO ANDREA; Sosso, Andrea; Febvre, Pascal; Shaternik, Volodymyr; Shapovalov, Andrii; Suvorov, Olexandr; Belogolovskii, Mikhail; Seidel, Paul. - In: IEEE TRANSACTIONS ON APPLIED SUPERCONDUCTIVITY. - ISSN 1051-8223. - 26:3(2016), pp. 1-5. [10.1109/TASC.2016.2535141]

Availability:
This version is available at: 11696/54570 since: 2021-03-05T17:27:06Z

Publisher:
IEEE

Published
DOI:10.1109/TASC.2016.2535141

(Article begins on next page)

Internally shunted Josephson junctions: a unified analysis

Vincenzo Lacquaniti, Cristina Cassiago, Natascia De Leo, Matteo Fretto, Andrea Sosso, Pascal Febvre, Volodymyr Shaternik, Andrii Shapovalov, Olexandr Suvorov, Mikhail Belogolovskii, Paul Seidel

Abstract— **Following the ever-rising demand for new functionalities and novel materials in superconducting circuitry, we provide a complete view on the self-shunting problem in Josephson junctions relating it to specific features of a multi-channel weak link between electrodes where averaging over the channels yields a bimodal distribution of transparencies with maxima near unity and zero. We provide two examples of such internally-shunted devices, four-layered Nb/Al-Al oxide-Nb junctions with strongly disordered nm-thick insulating layers where stochastic distribution of transparencies takes place on a local rather than a global scale and MoRe/W-doped Si-Si–MoRe devices with strongly inhomogeneous silicon interlayers partly doped by metallic nanoclusters where the main charge transport occurs across resonance-percolating trajectories. We show how the predicted universal distribution function of transmission coefficients can be verified experimentally without any fitting parameters and analyze some old and new experimental data from this perspective. We believe that our results can form a base for novel four-layered Josephson junctions with enhanced superconducting properties and, at the same time, well-separated metallic electrodes.**

***Index Terms*— Josephson junctions, Current-voltage characteristics, Tunneling, Charge carrier processes, Distribution functions.**

I. Introduction

The use of cryogen-free systems allows superconductive (S) devices to be far superior to other technologies not only for the advantages in speed and accuracy, but also from the viewpoint of energy efficiency. However, in order to exploit this, for instance, for computing and other high-impact applications, one has to develop a high-density technology which can cope with all basic requests that semiconducting technology is typically able to provide nowadays.

Among them, size, reproducibility, and uniformity represent today a limiting factor, but also other specific features such as the biasing current, the characteristic voltage of the device, and its stability must be improved.

Therefore, notwithstanding some excellent results in specific areas such as voltage standard and RSFQ circuits, where superconductive Josephson junctions are providing the best solution to some of the mentioned items [1], the research is still active to achieve an "ideal" basic element for superconductive active circuits.

Since for medium- to high-integration applications mentioned above one common desire is to have devices with non-hysteretic current-voltage (*I-V*) characteristics, intrinsic shunting of the barrier can achieve the objective, while keeping the size of the circuits as small as possible.

Junctions of this kind, using a normal-metal (N) layer as a barrier, have been made with a wide variety of non-superconducting materials. But in the SNS devices, due to the proximity effect, the near-interface superconducting properties in the S electrodes are strongly suppressed with the result that the I_cR_N products (I_c stands for the critical current and R_N is the normal-state junction resistance) nowadays are very low. Moreover, current-voltage characteristics of SNS devices can be hysteretic due to the increase of the normal-metal electron temperature once the junction switches to the resistive state [2]. It means that optimal Josephson junctions should be internally shunted like SNS trilayers but with insulating barriers without conducting electrons which can provide isolation between metallic electrodes.

To overcome this, two classes of junctions can be considered: (i) junctions with a specific transition region between the electrodes which includes a lot of transition channels with a broad spread of transmission probabilities D from near unity to almost zero and thus are shunted for intrinsic reasons and (ii) junctions where a metallic-to-insulator transition barrier is used, trimming its composition.

In the following, we discuss different types of non-hysteretic devices. Examples of type (i) are certainly double-barrier SINIS heterostructures with almost identical insulating (I) barriers [3,4]. In this case self-shunting appears due to the presence of transmission resonances in the transparency of the INI weak link between superconducting electrodes which are separated from the normal interlayer by insulating barriers [5].

Also asymmetric Nb/Al-AlO$_x$-Nb Josephson structures with ultra-thin oxide barrier which are not only intrinsically shunted but also possesses high temperature stability and good reproducibility are examples of this class [6-8].

In this contribution, we provide a more complete view on the self-shunting problem relating it to specific features of a multi-channel weak link between electrodes where averaging

V. Lacquaniti, C. Cassiago, N. De Leo, M. Fretto and A. Sosso are with the INRIM; National Institute for Metrological Research, Strada delle Cacce 91, 10135 Torino, Italy, e-mail: v.lacquaniti@inrim.it

V. Shaternik, A. Shapovalov, O. Suvorov and M. Belogolovskii are with Department of Superconducting Electronics, G.V. Kurdyumov Institute for Metal Physics, 03680 Kyiv, Ukraine, e-mail: belogolovskii@ukr.net

P. Febvre is with Université Savoie Mont Blanc, Campus scientifique, 73376 Le Bourget du Lac cedex, France, e-mail: pascal.febvre@univ-smb.fr

P. Seidel is with Low Temperature Group, Friedrich-Schiller-Universität Jena, Germany, e-mail: paul.seidel@uni-jena.de

over the channels yields a bimodal distribution of transparencies with maximums for D near unity and zero. Thus, intrinsic shunting is directly connected with the presence of a significant number of ‘open’ channels in a weak link between superconducting electrodes.

Besides the S/N-I-S four-layered structures [6-8], we discuss Josephson junctions where barriers are formed by silicon layers with embedded tungsten granules. In such devices the internal disorder of the barrier transparencies is caused by irregularly distributed metallic islands. Related experiments on self-shunted junctions of the two types are resumed and compared to the theory.

II. Bimodal Distribution Function for the Charge Transport Across Disordered Nanometer-Thick Insulating Films

In the following, we limit ourselves to structurally disordered nano-scaled insulating interlayers with preferably tunneling character of the transport and with a huge number of transport channels. Imagine that the transmission coefficient D in all channels has the same functional form with a single controlling parameter. Moreover, we assume that the parameter can be chosen so that its zero value corresponds to the maximum of the transparency D while D goes asymptotically to zero when the parameter increases infinitely (see the left side of Fig. 1). Next, we suppose that the governing parameter is almost uniformly distributed from very small to very large values. If so, the two flat regions of the curve will lead to two maxima in the distribution $\rho(D)$ of transmission probabilities (the right side of Fig. 1). One of them at $D = 1$ indeed means internal shunting of the sample. Thus, in spite of the evident individuality of the probability density function $\rho(D)$ for each sample, the problem is simplified by its inherent complexity which manifests itself in the large number of degrees of freedom in very strongly disordered dielectric layers and just in this case, as was argued in our previous papers [8,9], $\rho(D)$ may exhibit substantial universality.

In order to avoid shorts in the transport channels with $D \leq 1$ we proposed [6,7] to include an additional dirty normal-metal (N) interlayer with a finite transparency between the disordered ultra-thin insulating barrier and one of the electrodes. When $E_F >> U_0$ and $\kappa d << 1$, U_0 and d being the average barrier height and thickness, E_F and k_F are the Fermi energy and wave number in conducting electrodes, κ is the decaying length of the electron wave function in the barrier, the local transparency is the Lorentzian $D = 1/(1+Z^2)$ where the parameter $Z = \kappa^2 d/(2k_F)$ is further supposed to be a uniform random variable distributed from zero to infinity [9]. Then the disorder-averaged macroscopic conductance of the junction equals to $\bar{G} = \int_0^\infty \rho(Z)G(Z)dZ$ with a constant distribution function

$$\rho(Z) = 2\bar{G}/(\pi G_0) = \text{const} \qquad (1)$$

where $G_0 = 2e^2/h$ is the conductance quantum. Note that Eq. (1) does not depend on the complex structure of the tunneling barrier and, hence, is universal.

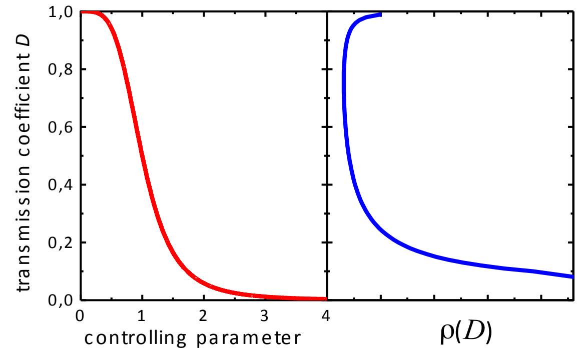

Fig. 1. Schematic of expected transparency-vs-controlling parameter dependence (the left side) and the related distribution function $\rho(D)$ (the right side).

Yet another example when the universal distribution function (1) can be realized is tunneling across insulating layers doped by conducting nano-scaled clusters. When the dopant concentration is not very small, peculiar resonance-percolation trajectories with periodic arrangement of nanograins with almost coinciding localized levels are formed inside the dielectric [10]. Calculations [11] for elastic tunneling through a single localized site within an insulating layer of comparatively thick barrier $\kappa d >> 1$ leads to the transparency which has a Lorentzian form for the difference between the incident electron energy and that of the resonance state. If the latter is distributed uniformly within a large energy interval we again get the same universal distribution function (1).

III. Charge Transport in S/N-I-S Junctions in the Quasi-Clean Limit

Our previous calculations of I-V curves in Nb/Al-Al oxide-Nb junctions [7,8] were based on the inequality $d_{Al} << \xi_{Al}^*$, where d_{Al} is the Al-interlayer thickness, $\xi_{Al}^* = \xi_{Al}\sqrt{T_{c,Al}/T_{c,Nb}}$, ξ_{Al} and $T_{c,Al}$ are the superconducting coherence length and critical temperature in Al, and $T_{c,Nb}$ is the critical temperature of Nb.

However, junctions with aluminum films more than 100 nm-thick, which are relevant for the increased temperature stability [12], do not fulfill the mentioned inequality and then we need a model valid in the opposite limit when d_{Al} is more than ξ_{Al}^* = 50-60 nm [7] and the Al film is non-superconducting. Notice that while the stepwise approximation for the pair potential in superconducting bilayers known as a rigid-boundary condition is not self-consistent, it captures main proximity-induced changes in the electronic density of states $N_N(E)$ of a normal metal caused by quasielectron-into-quasihole (and inverse) transformations of Bogoliubov quasiparticles at the N/S interface [13].

The next approximation used in [7,8] is connected with the electron mean free path l_{Al} in Al interlayers. In the bulk aluminum l_{Al} is the constant ~ 120 nm whereas in the films l_{Al} increases with film thickness and is of the order of d_{Al} since it is mainly limited by the surface scattering [14]. Thus, for $d_{Al} \geq$ 100 nm we have an intermediate situation between dirty and

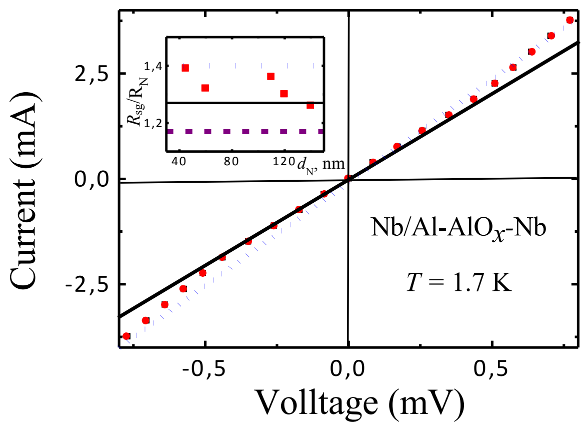

Fig. 2. The main panel: dissipative current–voltage characteristic of a representative Nb/Al–AlO$_x$–Nb junction with a 140 nm-thick Al interlayer at 1.7 K (squares); solid and dotted straight lines correspond to Ohm's laws with R_{sg} = 0.34 Ohm and R_N = 0.27 Ohm. The inset shows R_{sg}/R_N values for Al films with different thicknesses d_N; solid, dotted, and dashed lines correspond to theoretical values for S/N-I-S (quasi-clean limit, $d_{N/}= l_N$, $d_{N/}= 2\xi_N$*, this paper), N-I-S, and S/N-I-S (dirty limit with proximity-effect taken into account [8]), respectively.

clean limits. To take it into account, we have introduced an additional imaginary term $i/(2l_{Al})$ in the wave vector $k^{e(h)}$ of an electron (a hole) in the Al interlayer (see [15]).

The charge-transport problem in S/N-I-S junctions can be regarded as one-dimensional since the presence of the potential barrier drastically reduces the tunneling probability with increasing the incidence angle. We have calculated *I-V* curves for S/N-I-S four-layered junctions with arbitrary transparency *D* of the interspace between two superconducting electrodes. Our numerical simulations at zero temperature repeated in general terms similar calculations developed earlier [16-19] with the only exception, the presence of an additional phase shift originated from two passages across the N layer, first, as an electron (a hole) with an energy *E* and a wave vector $k^{e(h)}$ and, second, as a hole (an electron) after Andreev electron-into-hole (hole-into-electron) transformation. Related phase shifts are $\varphi^e = k^e d_N$ and $\varphi^h = -k^h d_N$ (note that the hole is moving in the direction opposite to that of its wave vector). Adding the phases we get the following relation for an additional phase shift induced by the presence of an N interlayer

$$\varphi = \left(k^e - k^h\right) d_N = 2\varepsilon d_N / \left(\hbar v_F\right) + i d_N / l_N \approx (\varepsilon / \Delta) d_N / \xi_N * + i d_N / l_N$$

here $\varepsilon = E - E_F$, v_F is the Fermi velocity. The proximized Al interlayer changes the probability amplitude of an Andreev-scattering process $\chi^{eh(he)}(\varepsilon)$=-arccos$\left(\varepsilon / \Delta\right)$ in a conventional s-wave superconductor [13] to $\tilde{\chi}^{eh(he)}(\varepsilon) = \varphi$-arccos$\left(\varepsilon / \Delta\right)$ and it is just the effect we are looking for.

The total quasiparticle current-vs-voltage characteristics of S/N-I-S heterostructures can be represented as a sum of independent contributions from individual transverse modes with a known distribution $\rho(D)$ of their transmission probabilities. Averaging the *I-V* curves for fixed parameters Z with the distribution function (1) we get an expected dissipative current-voltage characteristic for an S/N-I-S four-layered device with ideally disordered insulating barrier. Further, it will be characterized by the ratio of the subgap resistance $R_{sg}(\tilde{V}) = \tilde{V} / I_{qp}(\tilde{V})$ calculated at very low voltages $\tilde{V}$, to the normal-state resistance $R_N = 1/\bar{G}$ of the junction. Our numerical result $R_{sg}(\tilde{V}) / R_N = 1.27$ should be compared with related experimental data.

Measurements of *I-V* characteristics at 1.7 K have been carried out suppressing the critical current of the junctions with applied magnetic field, in an experimental apparatus already described in the previous paper [12]. The S/N-I-S junctions were fabricated as was reported earlier in Refs. 6-8. In order to test the new theoretical approach described above, junctions with an aluminum film as thick as 140 nm have been measured. Representative current-voltage characteristic is shown in the main panel of Fig. 2. Subgap ohmic resistance R_{sg} was extracted from experimental data as the slope of a best-fit linear regression line for quasiparticle curves in the interval from 0 to 0.2 mV where the subgap current increases linearly with *V* (the solid line in the main panel of Fig. 2). The normal-state resistance R_N was determined from a linear fit to dissipative current–voltage curves at ~ 1mV.

In the inset in Fig. 2 we compare experimental data for five different Nb/Al–AlO$_x$–Nb samples with the R_{sg}/R_N ratio values predicted for an N-I-S trilayer as well as for an S/N-I-S junction in the quasi-clean limit, this paper, and in the dirty proximity-effect limit, Refs. 7 and 8. It is evident that the novel model agrees better with experimental data, at least, for comparatively thick Al interlayers.

IV. Charge Transport in Josephson Junctions with Metallic Nanoislands Embedded into Low-Height Barriers

As was noted in the second section, superconducting junctions with low-height and, hence, comparatively thick insulating interlayers may be self-shunted by adding metallic nano-scaled drops into the barrier. First results on W-doped silicon (W:Si) interlayers in Josephson junctions formed by MoRe-alloy electrodes were published in Ref. 20. Below we present some new data and their theoretical interpretation valid at 4.2 K which corresponds to $T \approx T_c / 2$ in our samples.

In order to prevent direct transport between superconducting electrodes across regions with the transmission coefficient near unity we used an additional layer of Si with the thickness about 30-40 nm (we have found that neither junction resistance, nor superconducting characteristics were strongly affected by changing the Si thickness within this interval). In most samples, the current-voltage characteristics were non-hysteretic and all of them exhibited an excess current, a constant shift of the superconducting *I-V* curve towards that measured in the normal state at V exceeding Δ/e (the solid line in the main panel of Fig. 3). The ratio $I_c/I_{exc} \approx 2.4$ was found for the sample shown in Fig. 3. Now we show that just this ratio can serve as an indicator of the internal structure of a weak link in Josephson junctions.

Let us calculate its value at $T \approx T_c/2$. Temperature dependences of the Josephson critical current in SNS and SIS (with strongly disordered I barrier) trilayers were presented in Ref. 12. According to Ref. 21, the excess current for an SIS sandwich can be found by doubling the corresponding result for an NIS junction

$$I_{exc} = 2\int_{-\infty}^{\infty}\left[G_{NIS}(\varepsilon) - G_{NIN}\right]\left[f(\varepsilon - eV) - f(\varepsilon)\right]d\varepsilon \text{ .where}$$

$G_{NIS}(\varepsilon)$ and G_{NIN} are related differential conductances, $f(\varepsilon)$ is the Fermi function. In the absence of the barrier, at 4.2 K we get $I_c/I_{exc} \approx 1.3$. In the tunneling limit $D \ll 1$, $I_{exc} \to 0$ hence, $I_c/I_{exc} \to \infty$. Averaging related formulas with the distribution function (1) where we put $D_N = 1$, we have obtained $I_c/I_{exc} \approx 2.4$ at $T = 4.2$ K. In the inset in Fig. 3 we compare theoretical expectations and related experimental data for four samples with different dopant concentrations c_W. It follows from the data shown in the inset in Fig. 3 that the ratio I_c/I_{exc} increases with c_W as a result of the strong enhancement of the number of transport channels. But this conclusion is preliminary and should be confirmed by more detailed measurements.

Note that the product I_cR_N for the sample shown in Fig. 3 is of a comparatively large magnitude 3.8 mV. Sometimes we have even observed values several times higher. The nature of so large I_cR_N products still remains unclear.

V. Conclusion

The main aim of the paper was to show that internal shunting of Josephson junctions can be achieved using a strongly inhomogeneous insulating weak link with a bimodal transparency distribution $\rho(D)$ peaked at $D = 0$ and $D = 1$. We have discussed two possible ways to realize it, (i) an ultra-thin amorphous aluminum-oxide interlayer with very strong local fluctuations of the barrier height and thickness and (ii) comparatively thick semiconducting films with embedded metallic granulas. In the first case, the main mechanism of the charge transport is direct quantum tunneling through an inhomogeneous barrier while in the second case it is based on a quantum-percolation process including resonance trajectories with the transmission coefficient near unity.

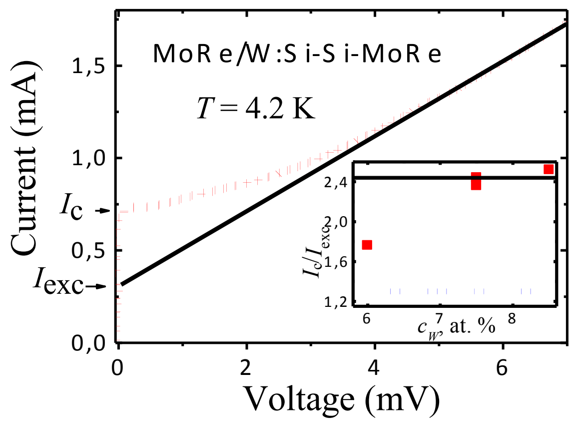

Fig. 3. The main panel: non-hysteretic *I–V* characteristic of a MoRe/W-doped Si–Si–MoRe junction with the dopant concentration 7.5 at% at 4.2 K, the thicknesses of the doped and undoped silicon interlayers were equal to 8 and 30 nm, respectively. Linear extrapolation shown by a solid line exhibits the presence of an excess current, arrows indicate critical supercurrent I_c and excess current I_{exc} values. The inset shows I_c/I_{exc} values for Si layers with different tungsten concentrations c_W; solid and dotted lines correspond to theoretical values of the ratio I_c/I_{exc} with a distribution function (1), see the text, and without any barrier, respectively, calculated at $T = T_c/2$.

We show how the predicted universal distribution function can be verified experimentally without any fitting parameters and analyze some old and new experimental data from this perspective. We compare theoretical results for the first-type Josephson devices with the data measured for Nb/Al–AlO$_x$–Nb four-layered junctions with more than 100 nm-thick aluminum interlayers and present some preliminary data obtained on MoRe/W:Si-Si-MoRe devices. We believe that these results can form a base for novel four-layered Josephson junctions with enhanced superconducting properties and, at the same time, well-separated metallic electrodes.

Acknowledgment

The authors are indebted to Elena Zhitlukhina for help in numerical calculations and Stefan Schmidt for stimulating discussions. One of us (M.B.) is thankful for the financial support from the grant No. 612600 LIMACONA "Light-Matter Coupling in Composite Nano-Structures", the EU Seventh Framework Programme. The work was partly supported by the German-Ukrainian project SE 664/18-1, Deutsche Forschungsgemeinschaft (DFG).

References

[1] H. G. Meyer, L. Fritzsch, S. Anders, M. Schmelz, J. Kunert, and G. Oelsner, "LTS Josephson junctions and ciruicts", in Applied superconductivity. Handbook on devices and applications. Vol. 1, Paul Seidel (Ed.), Wiley-VCH, 2015, pp. 281-305.

[2] H. Courtois, M. Meschke, J. T. Peltonen, and J. P. Pekola, "Origin of hysteresis in a Proximity Josephson Junction", Phys. Rev Lett., vol. 101, 067002, 2008 (4 pages).

[3] M. Yu. Kupriyanov, A. Brinkman, A. A. Glubov, M. Siegel, and H. Rogalla. "Double-barrier Josephson shvctures as the novel elements for superconducting large-scale integrated circuits", Physica C, vol. 326-327, pp. 16-45, 1999.

[4] A. Brinkman, D. Cassel, A. A. Golubov, M. Yu. Kupriyanov, M. Siegel, and H. Rogalla. "Double-barrier Josephson junctions: Theory and experiment", IEEE Trans. Applied Supercond., vol. 11, p. 1146-1149, 200I.

[5] A. A. Golubov, M. Yu. Kupriyanov, and E. Il'ichev. "The current-phase relation in Josephson junctions", Rev. Mod. Phys., vol. 76, p. 411-469, 2004.

[6] V. Lacquaniti, C. Cagliero, S. Maggi, and R. Steni, "Overdamped Nb/Al-AlO$_x$/Nb Josephson junctions," Appl. Phys. Lett., vol. 86, 042501, 2005 (3 pages).

[7] V. Lacquaniti, N. De Leo, M. Fretto, A. Sosso, and M. Belogolovski. "Nb/Al-AlO$_x$-Nb superconducting heterostructures: A promising class of self-shunted Josephson junctions", J. Appl. Phys. vol. 108, 093701, 2010 (8 pages).

[8] V. Lacquaniti, M. Belogolovskii, C. Cassiago, N. De Leo, M. Fretto, A. Sosso; "Universality of transport properties of ultrathin oxide films", New J. Phys., vol. 14, 023025, 2012 (13 pages).

[9] M. Belogolovskii. "Charge tunneling across strongly inhomogeneous potential barriers inmetallic heterostructures: A simplified theoretical analysis andpossible experimental tests", Appl. Surf. Sci., vol. 312, pp. 17–22, 2014.

[10] I. A. Devyatov and M. Yu. Kupriyanov. "Resonant Josephson tunneling through S-I-S junctions of arbitrary size", JETP , vol. 85, pp. 189–194, 1997.

[11] H. Knauer, J. Richter, and P. Seidel. "A direct calculation of the resonance tunneling in metal-insulator-metal tunnel junctions", Phys. Status Solidi A, vol. 44, pp. 303-312, 1977.

[12] V. Lacquaniti, D. Andreone, N. De Leo, M. Fretto, S. Maggi, A. Sosso, and M. Belogolovskii. "Analysis of the temperature stability of overdamped Nb/Al-AlO$_x$/Nb Josephson junctions", IEEE Trans. Applied Supercond., vol. 17, pp. 609-612, 2007

[13] M. Belogolovskii. "Proximity effect", in Applied superconductivity. Handbook on devices and applications. Vol. 1, Paul Seidel (Ed.), Wiley-VCH, 2015, pp. 49-65.

[14] A. Zehnder, P. Lerch, S. P. Zhao, T. Nussbaumer, E. C. Kirk, and H. R. Ott, "Proximity effects in Nb/Al-AlOx-Al/Nb superconducting tunneling junctions", Phys. Rev. B, vol. 59, pp. 8875-8886, 1999.

[15] F. Yang and R.-B. Liu. "Geometric diffusion of quantum trajectories", Sci. Rep., vol. 5, 12109, 2015 (9 pages).

[16] D. Averin D and A. Bardas. "ac Josephson effect in a single quantum channel", Phys. Rev. Lett., vol. 75, pp. 1831-1834, 1995.

[17] E. N. Bratus', V. S. Shumeiko, and G. Wendin. "Theory of subharmonic gap structure in superconducting mesoscopic tunnel contacts, Phys. Rev. Lett., vol. 74, pp. 2110-2113, 1995.

[18] M. Hurd, S. Datta, and P. F. Bagwell. "Current-voltage relation for asymmetric ballistic superconducting junctions", Phys. Rev. B, vol. 54, pp. 6557-6567, 1996.

[19] M. Hurd, T. Löfwander, G. Johansson, and G. Wendin." ac Josephson effect in superconducting d-wave junctions", Phys. Rev. B, vol. 59, pp. 4412–4426, 1999.

[20] V. Shaternik, A. Shapovalov, M. Belogolovskii, O. Suvorov, S. Döring, S. Schmidt, and P. Seidel. Transition from Coulomb blockade to resonant transmission regime in superconducting tunnel junctions with W-doped Si barriers", Mater. Res. Express, vol. 1, 026001, 2014 (10 pages).

[21] G. E. Blonder. M. Tinkham, and T. M. Klapwijk. "Transition from metallic to tunneling regimes in superconducting microconstrictions: Excess current, charge imbalance, and supercurrent conversion", *Phys. Rev. B*, vol. 25, pp. 4515-4532, 1982.